JOURNAL OF MATERIALS SCIENCE 8 (1973) 1349–1354

A preliminary study of dislocations in indium and gallium phosphides

R. C. CLARKE, D. S. ROBERTSON, A. W. VERE
Royal Radar Establishment, Great Malvern, Worcs, UK

The determination of dislocation densities and distributions in III-V compounds by etching techniques frequently leads to erroneous results, especially where high densities are involved. The paper reports the use of a HNO_3:HCl:Br etch on slices of InP and GaP and specifies the conditions under which the etch may be used as a precise guide to the dislocation density and distribution.

Comparison of etch-pit micrographs and X-ray Lang topographs is used to establish the validity of the etching technique and to obtain information on the type, density and distribution of dislocations in substrates and epitaxial layers.

1. Introduction

Although no clear picture has yet emerged of the role of dislocations in determining the efficiency of electronic devices in III-V compounds, considerable effort has been devoted to the topic [1, 2], Several techniques are available for obtaining information on dislocations, but no one technique has proved entirely satisfactory. Electron microscopy, for example, provides details on Burgers vectors and dislocation strain fields but is only useful for examining dislocation densities which exceed 10^6 cm^{-2}. Even then, the thinning procedures required may lead to erroneous density estimates. X-ray topography [3], in contrast, affords a non-destructive technique for lower resolution evaluation of much lower densities over much larger specimen areas. Here the disadvantage lies in the long exposure times required. The simplest method, and that most frequently used, is to reveal dislocations by surface etching, but extreme caution must be used in the interpretation of the results to ensure that the etch pits revealed are attributable to dislocations and that allowances are made for dislocations lying parallel or slightly inclined to the etched surface. Our studies on indium phosphide show that the conventional guidelines which indicate a correlation between etch pits and dislocations (e.g. occurrence of identical etch pit configurations on opposite surfaces of slices or the presence of pairs or rows of pits indicating isolated loops or slip lines) may be absent, even when the dislocation density exceeds 10^3 cm^{-2}. In this work, therefore, considerable attention has been given to developing a reliable etchant and etching procedure and to comparing results obtained in this way with transmission X-ray topographs of the same regions of the specimen.

During the course of this study much information was gained on the nature and distribution of dislocations in InP, in both substrates and epitaxial layers. The dislocation density and distribution in Czochralski-grown material is determined by the thermal stresses imposed during cooling and any subsequent mechanical deformation. An analysis of the former [4] suggests that when radial hoop stresses predominate during cooling from the melt the resultant dislocation density is highest at the outer surface of the crystal, decreases to a minimum at approximately $R/2$, where R is the crystal radius, and rises slightly at the centre of the crystal. This type of distribution is frequently encountered in InP crystals.

2. Experimental procedure

Czochralski grown [5] [111] and [100] axis single crystals of InP and GaP crystals were cut to produce (100) slices approximately 0.5 mm thick. The slices were then etch-polished to remove 100 μm from both faces using a 2% Br-CH_3OH solution for InP or a 5% Br-CH_3OH solution for GaP. The etchant used to reveal dislocations and other defect structures consisted of conc.HCl, conc.HNO_3 and bromine in the

© *1973 Chapman and Hall Ltd.*

volume ratio 20:10:0.25. This etch functions satisfactorily after a 5 min induction period and is effective for approximately 4 h. The etch was found to be effective on {100} and {111} faces, but unreliable results were obtained during the etching of {110} faces. The maximum etching times used were 5 sec for {111} InP and 60 sec for {100} InP. For GaP the corresponding maximum etching times were 60 and 120 sec.

For X-ray transmission Lang topographs the specimen slices were thinned to approximately 100 μm by free etching in 2% $Br\text{-}CH_3OH$ solution, after initial etching-polishing as described above. Topographs were produced using a conventional Jarrel-Ash Lang camera with $AgK\alpha_1$ radiation. The diffracting conditions used are indicated on the appropriate topographs.

The dislocation densities were calculated from optical micrographs by counting etch-pits per unit area and from X-ray topographs by counting the number of intersections of dislocation lines with the foil surfaces. In the latter case, the value is divided by two to determine the number of dislocation emergence points per surface.

Examinations have also been conducted on vapour grown epitaxial layers. The growth of these layers has been described in a previous publication [6].

3. Results and discussion

Before considering the type and distribution of dislocations in III-V compounds, it is necessary to ensure that the etching procedure chosen gives a 1:1 correlation between surface etch-pits and dislocations. Fig. 1a is an optical micrograph of an etched (100) surface of an InP slice cut from a [100] axis crystal. The corresponding transmission X-ray topograph is shown in Fig. 1b. Both micrographs indicate that the dislocation density at the upper edge of the slice (which corresponds to an external surface of the original crystal) is approximately 10^5 cm^{-2} and reduces to 5×10^3 cm^{-2} towards the interior of the original crystal. The optical micrograph also shows growth striae with a periodicity of approximately 0.3 mm. It is interesting that the striae are not visible on the X-ray topographs despite the fact that the vector product of the diffraction vector and the strain vector associated with growth striae is non-zero. In silicon and GaAs the strains associated with growth striae are easily detectable on X-ray topographs.

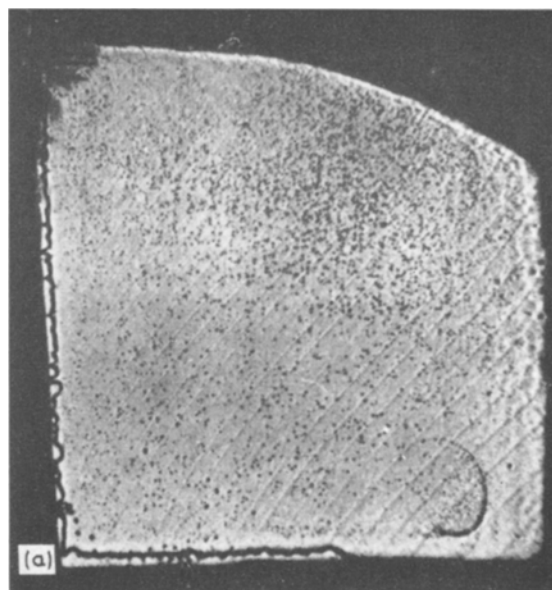

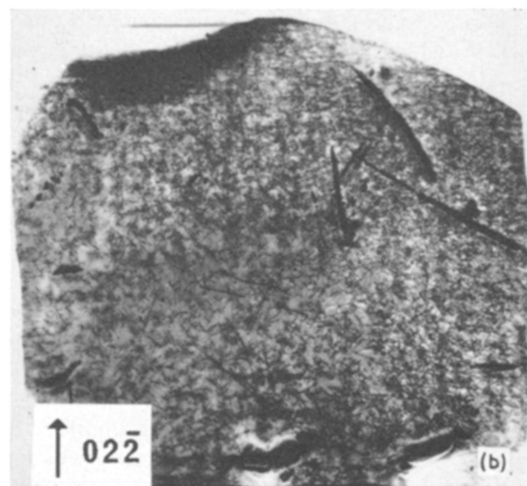

Figure 1 (a) Optical micrograph (× 12.5) of an etched (100) slice of InP. (b) Transmission X-ray topograph of the same slice.

The X-ray topograph also shows a series of high intensity, sharply defined lines identified as surface scratches and an elastically strained region (no contrast region) probably attributable to the specimen mounting.

The essential result of the comparison of the optical micrograph and the topograph is the conclusion that the etch pit distribution may be used as a reliable guide to the density and distribution of dislocations within the slice. Whether or not the correlation is truly 1:1 is

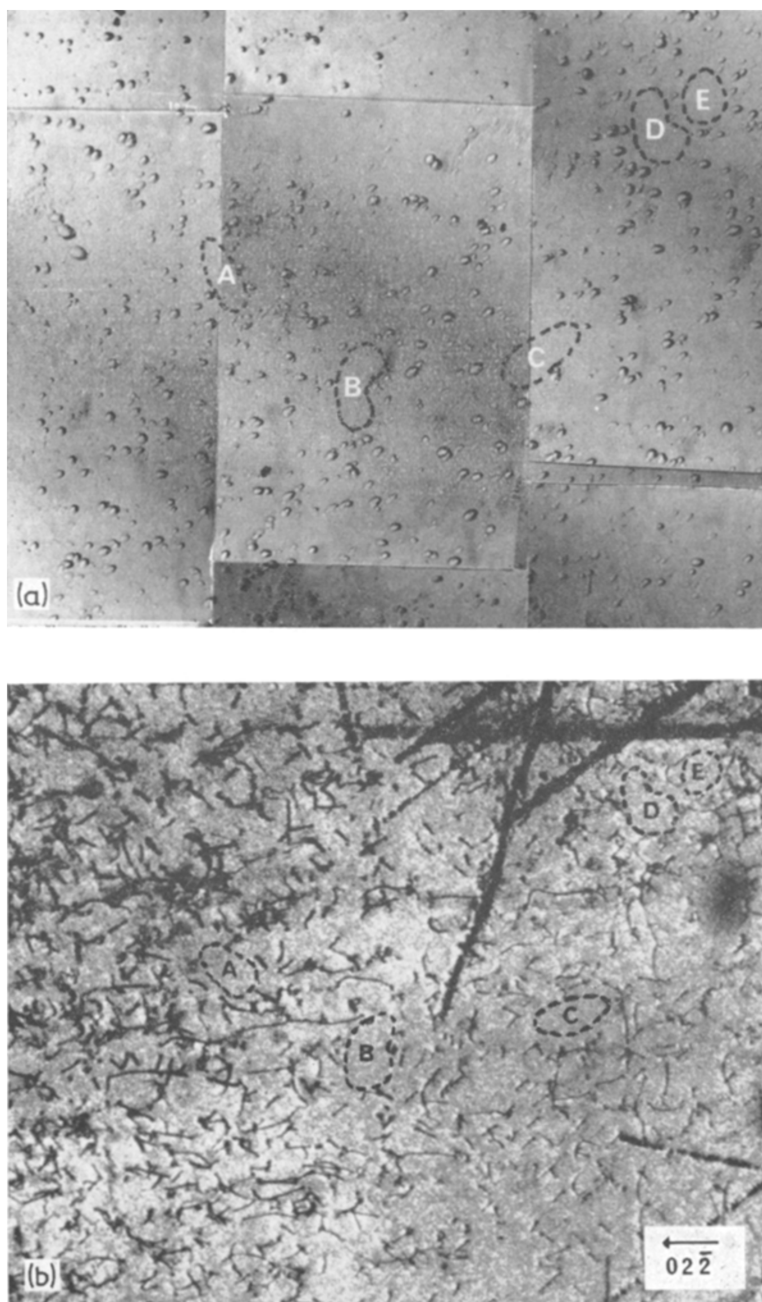

Figure 2 Comparison of a high magnification (× 35) micrograph (a) and a topograph (b) of the same area of a (100) InP plane.

difficult to establish in material of this dislocation density. Fig. 2 shows a high magnification comparison between a micrograph and a topograph of the same area of a (100) InP slice. The correlation between the two photographs is not immediately obvious, but can be seen more clearly by comparing the location of low dislocation density areas in each field of view. Equivalent areas are marked to aid comparison. A more precise comparison, obtained using a

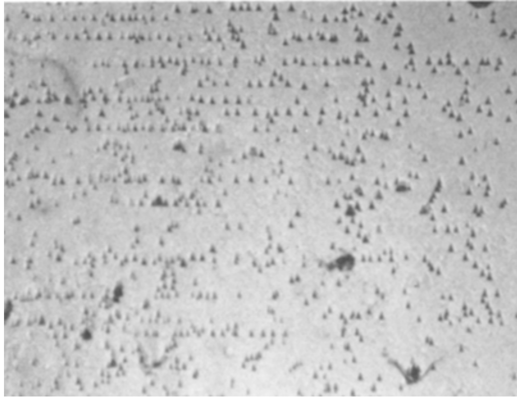

Figure 3 A {1 1 1} InP plane showing dislocation etch pits defining [0 1 1] slip lines (× 47).

transparent overlay, confirms that the emergence points of dislocation lines are identified by etch pits. The etch pits are not crystallographic in nature and appear asymmetric, the long axis of the pit lying along the direction of the projection of the dislocation line onto the surface plane. In addition to these etch-pits, the micrographs shows a series of smaller, flat-bottomed pits which are not associated with dislocation lines. Since these are much fewer and fainter than the dislocation etch pits their occurrence does not significantly affect estimates of dislocation density based on etch-pit counts. The origin of the fainter, flat-bottomed pits has not yet been positively identified, although it is possible that they are due to precipitation.

{1 1 1} slices of InP show crystallographic etch pits with ⟨1 1 0⟩ edges (Fig. 3). Again the distribution of etch pits and dislocations is comparable in micrographs and topographs of the same area. In this case however, an etch pit count leads to an underestimation of the dislocation density since many of the dislocations

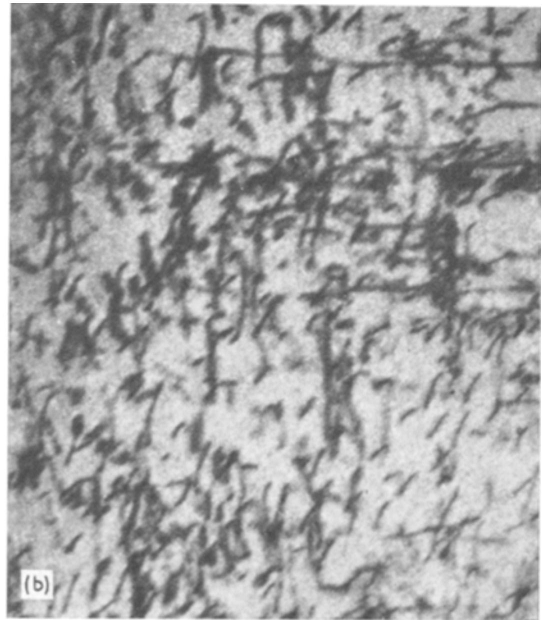

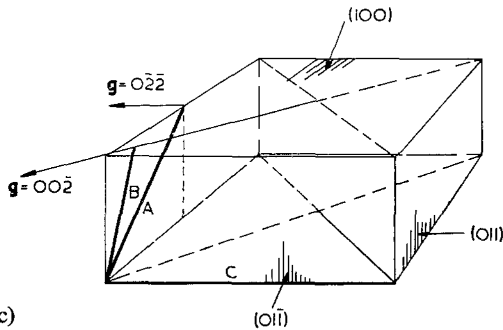

Figure 4 (a) X-ray topograph of a (1 0 0) InP slice g = $0\bar{2}\bar{2}$. (b) The same area with g = 0 0 2 (× 47). (c) Schematic diagram of the dislocation geometry.

lie on (1 1 1) planes parallel to the specimen surface and are not therefore revealed by etching. Further information on the dislocations visible in InP substrates has been obtained by studying topographs of the same area of a (1 0 0) slice taken under different diffraction conditions (Fig. 4).

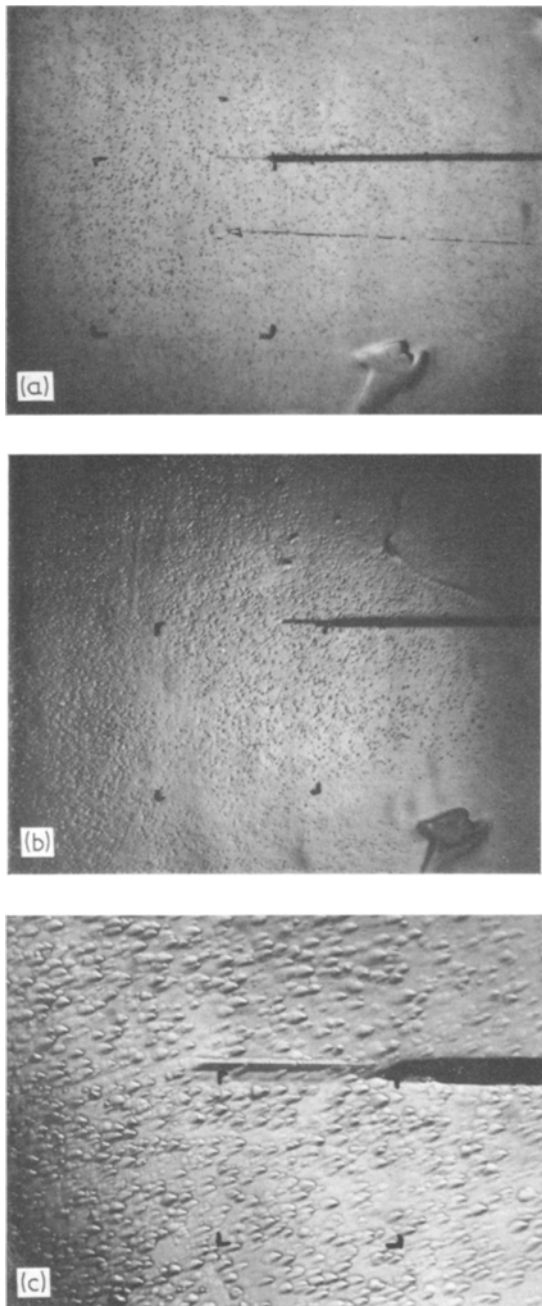

Figure 5 Micrographs showing variation in etch pit density as a function of depth in an InP device. (a) At surface of a 6.3 μm epitaxial layer (× 21). (b) After removal of 3 μm (× 21). (c) After removal of the complete layer to reveal the substrate (× 84).

The dislocations lie predominantly in three directions illustrated schematically in Fig. 4c. The three types of dislocation have been designated A, B and C. From a knowledge of the foil thickness (120 μm) and the projected lengths and directions of the dislocation lines on the (100) surface it is seen that type A dislocations lie along $[21\bar{1}]$ directions while type C lie along [011] directions. Both these directions are contained within the $(1\bar{1}1)$ plane, which is the most commonly occurring slip plane in Si, Ge and III-V compounds. Slip line directions on {100} and {111} surfaces further confirm the occurrence of slip on {111} planes in InP. Type B dislocations lie in directions more steeply inclined to the foil surface but are not confined to any specific low index direction, indicating that they have undergone climb during the post-growth annealing period.

The intensity of a dislocation image is dependent upon the relationship between the Burgers vector of the dislocation and the diffraction vector **g** denoting the normal to the Bragg-reflecting crystallographic planes. Thus, for screw dislocations the image intensity is greater when **g** is parallel to ***b*** and reduces to zero when $\mathbf{g}.b = 0$. For edge dislocations, the image contrast is maximum when **g** is parallel to ***b*** and minimum, though not completely eliminated when $\mathbf{g}.\boldsymbol{b} = 0$. Close examination of Fig. 4 shows that the image intensity of type A dislocations is greatly reduced when $\mathbf{g} = 002$, indicating a Burgers vector perpendicular to [001], whereas type B dislocations become invisible under $\mathbf{g} = 0\bar{2}\bar{2}$ indicating a Burgers vector perpendicular to $[0\bar{1}\bar{1}]$.

The type C dislocations remain visible under both diffracting conditions. Moreover, type C dislocations have only been observed in specimen slices composed of both substrate and epitaxial layer. This fact, together with their geometrical alignment suggests that they are mismatch dislocations associated with the layer-substrate interface. It should be emphasized that device slices do not always show this type of dislocation. For example, Fig. 1, which is a transmission topograph of a vapour-deposited 15 μm layer on a 100 μm substrate shows no evidence of type C dislocations.

In order to study the propagation of dislocations from the substrate into the epitaxial layer in InP, a 6.3 μm thick layer was vapour deposited on a Sn-doped substrate. (The free carrier concentrations of the layer and substrate at 298 K were 1.2×10^{15} and 2×10^{18} respectively. Fig. 5a shows the etch-pit density recorded at the layer surface and Fig. 5b, that obtained after

removal of 3 μm of the layer using the 2% Br:CH_3OH free-etch. In each case the density is 6×10^4 cm^{-2}. The layer was then completely removed and the underlying substrate re-etched, to reveal a dislocation density of 1.8×10^5 cm^{-2} (Fig. 5c).

Since interface mismatch dislocations or other dislocations lying in the interface plane would not be revealed by the etch, this one third drop in density cannot be attributed to the non-propagation of type C dislocations and implies that even dislocations inclined at comparatively large angles to the interface plane may not propagate into the layer. This behaviour is not fully understood and is the object of further investigation.

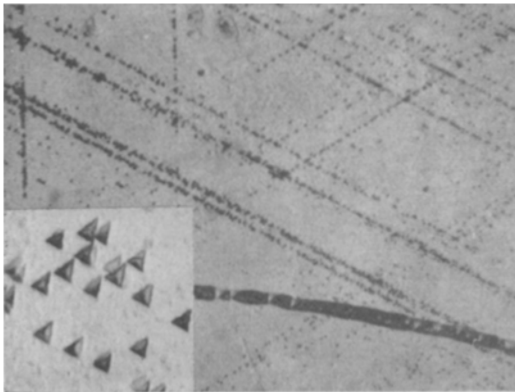

Figure 6 Etch pits delineating {111} slip in GaP (× 46). Inset: high magnification micrograph showing etch pit details (× 300).

Finally, it should be noted that the use of the HCl:HNO_3 Br etch to reveal dislocations has also been successfully carried out on {100} and {111} slices of GaP. Fig. 6 shows slip bands on a (111) GaP surface. The orientation is identical to that previously reported by Saul [7]. The etch pits are again bounded by ⟨110⟩ directions and have a side length of 10 μm.

4. Conclusions

1. The 20 HCl:10 HNO_3:0.25 Br etch, when freshly made, produces etch pits on (100) slices of InP, GaAs and GaP, which show good correlation with the underlying dislocation structure. Smaller, less well defined etch pits, apparently not related to dislocation emergence sites are also observed, but these do not greatly affect dislocation density estimates.
2. Dislocations intersecting the surface are also revealed when etching {111} surfaces with this etch, but the presence of dislocations lying parallel to the surface leads to an underestimation of dislocation density from etch pit counts.
3. The dislocation distribution in InP substrates is entirely consistent with that attributed by Penning to dislocation generation by the radial thermal stress during cooling from the melt.
4. The dislocation density in bulk InP currently in use ranges from 5×10^3 cm^{-2} to $> 10^5$ cm^{-2}.
5. The dislocation density in epitaxial layers is approximately one third that of the substrate.

Acknowledgements

The authors would like to express their thanks to their colleagues in the Physics and Electronics Groups for their interest in, and comments on, this work and particularly to Mrs L. L. Taylor for preparing specimens for evaluation. The paper is contributed by permission of the Director of RRE and published by permission of HMSO.

References

1. W. E. TAYLOR, W. C. DASH, B. E. MILLER, and C. W. MULLER, "Properties of elemental Compound Semiconductors", Ed. M. C. Gatos (Interscience, New York, 1960) p. 337.
2. M. S. ABRAHAMS and C. J. BUIOCCHI, *J. Appl. Phys.* **37** (1966) 1973.
3. E. S. MEIERAN, *Siemens Rev. 4th Special Issue* **37** (1970) 39.
4. P. PENNING, *Philips Res. Rept.* **13** (1958) 79.
5. J. B. MULLIN, R. J. HERITAGE, C. H. HOLLIDAY, and B. W. STRAUGHAN, *J. Crystal Growth* **3, 4** (1968) 281.
6. R. C. CLARKE, B. D. JOYCE, and W. H. E. WILGOSS, *Solid State Communications* **8** (1970) 1125.
7. R. H. SAUL, *J. Electrochem. Soc.* **115** (1968) 1184.

Received 20 February and accepted 22 March 1973.